

Jun.2010 / Vol.130

MITSUBISHI ELECTRIC

# ADVANCE

Core Technologies for Creating a Low-carbon Society

• **Editorial-Chief**

*Kiyoshi Takakuwa*

• **Editorial Advisors**

*Masujima Toshio  
Kanae Ishida  
Makoto Egashira  
Tetsuji Sorita  
Hiroaki Kawachi  
Masayuki Masuda  
Takahiro Nishikawa  
Tetsuyuki Yanase  
Ichiro Fujii  
Taizo Kittaka  
Keiji Hatanaka  
Daisuke Kawai  
Hideyuki Ichiyama  
Kazumasa Mitsunaga*

• **Vol. 130 Feature Articles Editor**

*Motohiro Tanaka*

• **Editorial Inquiries**

*Makoto Egashira  
Corporate Total Productivity Management  
& Environmental Programs  
Fax +81-3-3218-2465*

• **Product Inquiries**

*Motohiro Tanaka  
Corporate Environmental Sustainability  
Group  
Fax +81-3-3218-2465*

**Mitsubishi Electric Advance** is published on line quarterly (in March, June, September, and December) by Mitsubishi Electric Corporation.  
Copyright © 2010 by Mitsubishi Electric Corporation; all rights reserved.  
Printed in Japan.

**CONTENTS**

**Technical Reports**

Overview .....1  
*by Hisashi Shiota*

The 6th Environmental Plan and Reduction in CO<sub>2</sub> from Production by Expanding Production Line Improvements .....2  
*by Hisashi Shiota*

Photovoltaic Power Generation Systems  
– Advanced Technologies for Producing Solar Cells – .....6  
*by Takashi Ishihara and Hiroaki Morikawa*

Energy Conservation and Resource Saving via SiC Inverters ...10  
*by Shin-ichi Kinouchi and Shuhei Nakata*

Lineup and Features of Air-to-Water Products for Europe .....13  
*by Yoshihiro Takahashi*

# Overview



Author: *Hisashi Shiota\**

## Reaching the 200 Year Mark – Looking Ahead to Becoming a Leading Environmental Brand

In its Environmental Vision 2021, the Mitsubishi Electric Group has set two objectives: to be recognized by society as an environmentally advanced company, and to build a corporate culture and capability as a “bicentennial enterprise” to ensure that our sustainable business activities continue for many years to come.

Toward this goal, we continue to work on reducing production costs by decreasing the amount of CO<sub>2</sub> emissions from production and the level of resource inputs. We are also supporting efforts to reduce CO<sub>2</sub> in the residential and transportation sectors by greatly improving the energy-saving performance of our products, which in turn boosts our business. In addition, we are conducting our own activities to preserve biodiversity.

Through these efforts, the Mitsubishi Electric Group strives for environmental compatibility by mitigating global warming and creating a recycling-based society, while strengthening its corporate competitiveness.

# *The 6th Environmental Plan and Reduction in CO<sub>2</sub> from Production by Expanding Production Line Improvements*

Author: *Hisashi Shiota\**

## **1. Introduction**

In April 2009, the Mitsubishi Electric Group launched its 6th Environmental Plan, which sets the targets and action plans for the three-year period FY2010–2012 to attain the goals of Environmental Vision 2021. This plan was developed focusing on consistency between the environmental performance targets and Environmental Vision 2021, expansion of global environmental management, and businesses related to tackling global warming.

Reducing CO<sub>2</sub> emissions from production is a priority activity for preventing global warming. We have set a total reduction amount as the goal of this activity, rather than the conventional reduction per unit. In order to improve the production lines, in addition to increasing efficiency and improving operation of utility devices, we will enhance measures that identify and eliminate hidden energy losses.

Based on the belief that a production system requiring less resources and energy also raises productivity and strengthens the corporate culture and capability, the Mitsubishi Electric Group strives for environmental compatibility and fulfilling its corporate responsibilities as a global operation by helping to create a sustainable society by expanding environment-related businesses that tackle global warming.

## **2. Body**

From 1998 to 2005, the atmospheric CO<sub>2</sub> concentration increased annually by an average of 2 ppm, and is currently about 380 ppm. The Intergovernmental Panel on Climate Change (IPCC) presented a set of scenarios in which the threshold accumulation of CO<sub>2</sub> is 400 ppm and the concentration is stabilized at that level. To make this happen, it was estimated that the CO<sub>2</sub> emission level would peak by 2015 and global CO<sub>2</sub> emissions in the year 2050 would be reduced by –50% to –85% from the 2000 level. If this scenario becomes a reality, the manufacturing industry including Mitsubishi Electric must be able to survive the competition and stay in business with lower CO<sub>2</sub> emissions. In other words, production with lower CO<sub>2</sub> emissions requires developing a production system that uses less re-

sources and energy, which in turn equals increased productivity and strengthened corporate culture and capability.

Announced in October 2007, Environmental Vision 2021 establishes the framework for long-term environmental management by the Mitsubishi Electric Group, striving to prevent global warming and to build a recycling-based society. The objective of this vision is to realize both environment-friendly and environment-compatible management, by setting target values including a 30% reduction of total CO<sub>2</sub> emissions from production by FY2021, in view of the target 50% reduction of global CO<sub>2</sub> emissions by 2050. In addition, since April 2009, the 6th Environmental Plan (FY2010–2012) has been carried out towards achieving Environmental Vision 2021 by defining target values and action plans for enhanced environmental performance. This plan aims to build a sustainable society by responding to social changes and needs concerning environmental problems, as well as by expanding environment-related businesses.

This paper summarizes our current key activities for improving the production lines to reduce their CO<sub>2</sub> emissions.

## **3. Reducing CO<sub>2</sub> from Production**

Figure 1 shows the plan for reducing total CO<sub>2</sub> emissions from production by all group companies. The data is compiled for the base year, and the target years of the 6th Environmental Plan (FY2012) and Environmental Vision 2021 (FY2021) by summing up the amount of CO<sub>2</sub> emissions from Mitsubishi Electric Corporation alone, its affiliates in Japan, and its overseas affiliates. In the 6th Environmental Plan, the emission reduction is set at 18%, down to 930,000 tons from the base year level, and the breakdown is as follows: Mitsubishi Electric alone: 24% or 510,000 tons; affiliates in Japan: 18% or 190,000 tons; and overseas affiliates: 4% or 230,000 tons reduction. These figures are based on the increase/decrease of CO<sub>2</sub> emissions estimated by taking into account the production slowdown caused by the economic slump in late 2008 and the forecast for growth in environment-related businesses such as

photovoltaic power generation systems, and the expected CO<sub>2</sub> reduction from existing facilities and by each type of business.

#### 4. Reducing CO<sub>2</sub> from Product Usage / Reducing Level of Resource Inputs

The amount of CO<sub>2</sub> from product usage is defined as the equivalent CO<sub>2</sub> emission converted from the energy consumed when the product is used by the customer. The amount of CO<sub>2</sub> from the use of Designed for the Environment (DfE) products shipped in FY2009 is estimated as 3.6 million tons a year. Assuming that the average service life of these products is 15 years, the total CO<sub>2</sub> emitted during their use would be 54 million tons.

The amount of CO<sub>2</sub> emissions from production by the Mitsubishi Electric Group in FY2009 was 948,000 tons, and thus the CO<sub>2</sub> from product usage is much greater than that from production. Therefore, reducing

CO<sub>2</sub> emissions from the usage of our products (amount of consumed energy) will help cut global CO<sub>2</sub> emissions. The Mitsubishi Electric Group has been working on DfE products to reduce the total environmental load throughout the product lifecycle. Figure 2 shows some examples of the reduction technologies and product names. Since a number of factors, such as the timing of introducing the reduction technology, differ for each product type, the target values in FY2012 against the base year for the reduction of CO<sub>2</sub> emissions from product usage also differ accordingly. Considering this difference, we calculated two hypothetical values for the accumulated CO<sub>2</sub> emissions from product usage: one with the CO<sub>2</sub> emissions from product usage in the base year and the other in the target year. We calculated a reduction rate using these two hypothetical values as the average reduction rate of all product types, which was then set as the target value for FY2012. Figure 3 shows the expected reduction of CO<sub>2</sub> emissions from

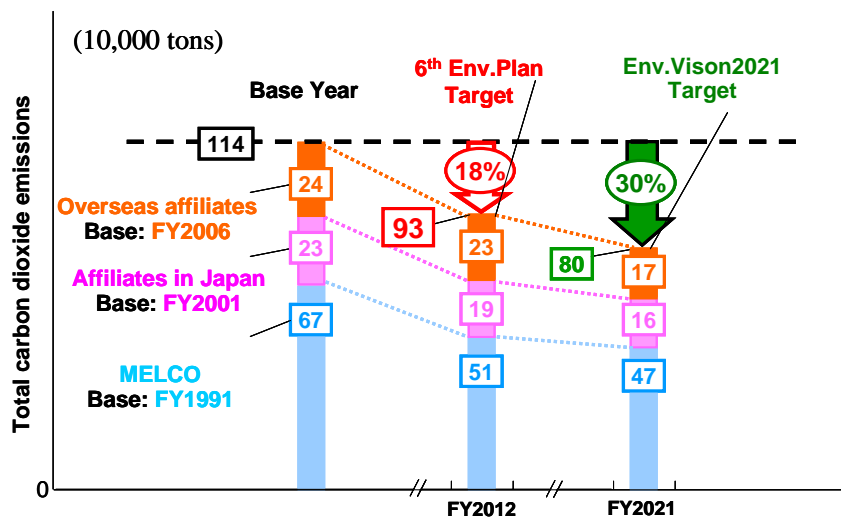


Fig. 1 Reducing total carbon dioxide emissions from production

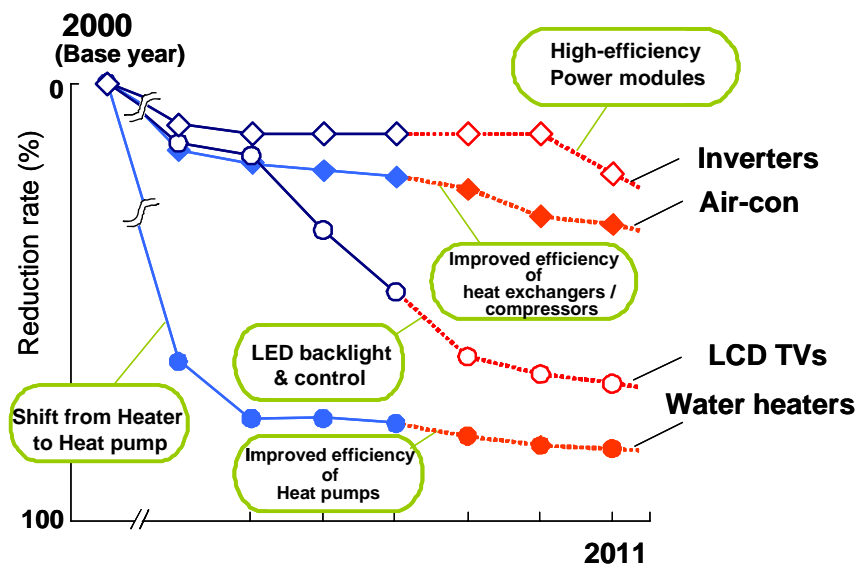


Fig. 2 Reduce CO<sub>2</sub> from product usage with eco technology

product usage in the 6th Environmental Plan.

Aiming at the target of Environmental Vision 2021 for reducing CO<sub>2</sub> emissions from product usage (30% reduction in FY2021 from FY2001 as the base year), the 6th Environmental Plan set a target average reduction of CO<sub>2</sub> emissions from using the subject products at 25%, and increased the subject products from the current 43 to 80.

When recycled resources are used extensively to cope with the dwindling resources of crude oil, mineral ores and other natural resources, the recycling itself requires energy. That is, energy is required to produce raw materials needed for producing end products, and to reduce CO<sub>2</sub> emissions from the production of raw materials, the amount of raw materials produced must also be restricted. One approach is to make the end products smaller and lighter. Environmental Vision 2021 sets a target of a 30% reduction in resource inputs from the FY2001 level. Toward this goal, as shown in Fig. 4, the 6th Environmental Plan aims to reduce the level of resource inputs by making the end products smaller and lighter. The target is an 18% reduction by FY2012 using an index of the average reduction rate in resource inputs for the target end products.

**5. Expansion of Businesses Related to Tackling Global Warming**

Products and services that can help reduce global CO<sub>2</sub> emissions include high-efficiency end products,

control equipment, and information systems for environmental information management and analysis in product categories such as air conditioners, lighting fixtures, and power equipment. This area is defined as “businesses related to tackling global warming”. We plan to expand this business to achieve sales of over 1.3 trillion yen in FY2016, and we estimate that these products can reduce global CO<sub>2</sub> emissions by about 5.1 million tons per year. Among the products, photovoltaic generation systems would account for sales of 250 billion yen and CO<sub>2</sub> reduction of 0.35 million tons.

**6. Expansion of High-efficiency, Clean Power Generation Facilities**

To reduce CO<sub>2</sub> in the power generation business, we intend to expand the supply of high-efficiency, clean (low CO<sub>2</sub> emission) power generation facilities, including nuclear power, combined cycle thermal power, hydro power and photovoltaic power generation facilities. We delivered the first high-efficiency facilities in FY2001, and installed facilities will reduce CO<sub>2</sub> by some 90 million tons by FY2021.

**7. Production Line Improvements for Reducing CO<sub>2</sub> Emissions**

Activities for reducing CO<sub>2</sub> emissions from production are divided into two main groups: those for increasing efficiency and improving operation of utility devices such as air conditioners, lighting fixtures, boil-

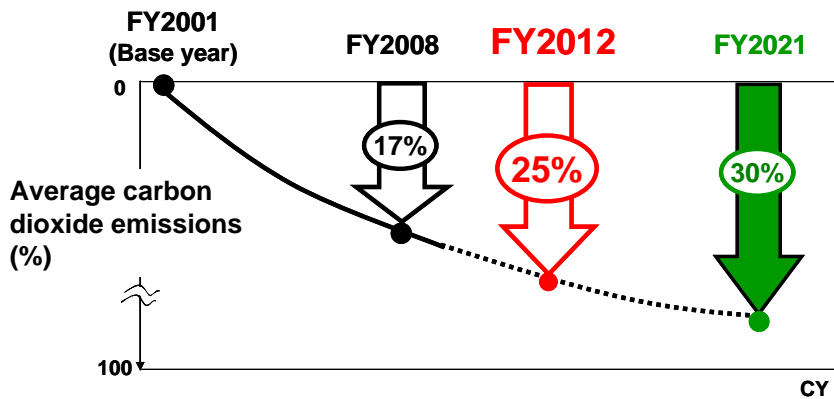


Fig. 3 Reducing carbon dioxide emissions from product usage

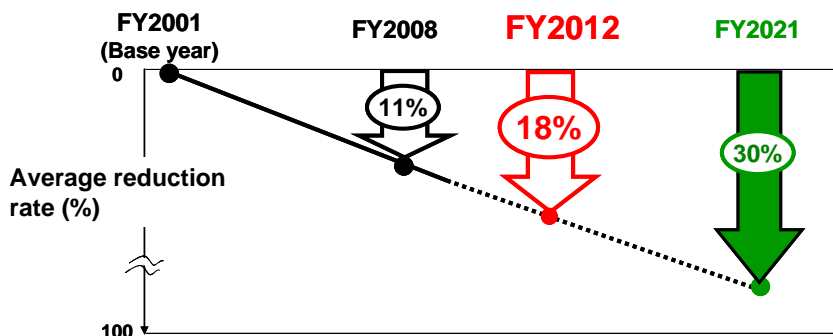


Fig. 4 Reducing resource inputs by making products smaller and lighter

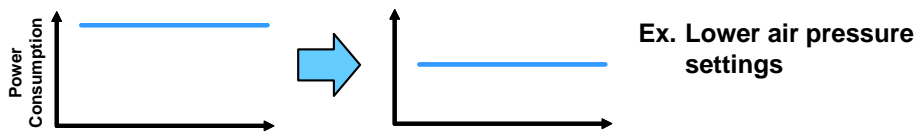
ers, compressors, receiving and transforming facilities; and those for production line improvements that collectively refer to improvement activities in various processes including surface treatment such as painting and plating, cutting and other machining works, and heat treatment such as annealing and quenching, welding, soldering, assembling, transferring, testing and inspection. The CO<sub>2</sub> reduction results for Mitsubishi Electric during the three years from 2005 to 2007 indicate that reductions from production line improvements are one-third to one-half the reductions from increasing the efficiency and improving the operation of utility devices. The 6th Environmental Plan will further reduce CO<sub>2</sub> from production by improving production lines.

Collectively called "production line improvements", the measures cover a wide variety of processes, each of which requires its own improvement method. Figure 5 shows some examples of those methods: decreasing the output level (base level) by lowering the setting pressure of pneumatically or hydraulically driven press machines (for example, reducing pressure loss by eliminating leaks or shortening the pipe length); chang-

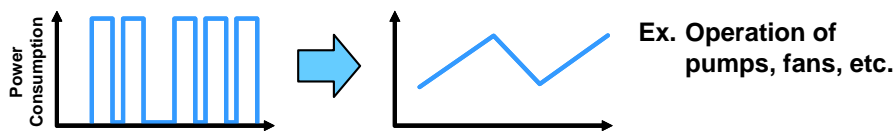
ing the ON-OFF control to inverter control for the motor of cooling pumps, fans, etc.; and turning off the power of electric furnaces when idle.

In each of these cases, the energy usage of production lines was analyzed, and unnecessary losses were identified by comparing the results with the corresponding production volume, etc. It was found that CO<sub>2</sub> can be reduced by avoiding unnecessary energy consumption hidden in the production process. In addition, once the productivity level is improved and stabilized, the number of defective products will be reduced, thus saving the energy required for producing and repairing those defective products. When modifying the production process conditions for improving productivity and/or reducing CO<sub>2</sub> emissions, any changes to empirical conditions, especially those related to product quality control, require thorough preparation. Focusing on high energy-consuming thermal processes such as baking, annealing, quenching and drying, we will continue to identify and eliminate unnecessary losses while improving both quality and productivity.

■ **Decreasing output levels (base levels)**



■ **Utilization of inverters**



■ **Prevention of idling line operation**

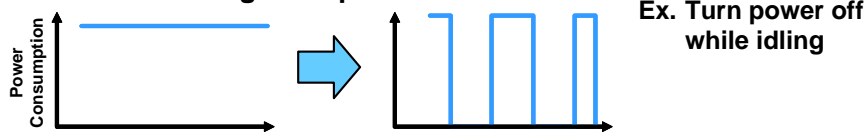


Fig. 5 Production line improvements

# Photovoltaic Power Generation Systems – Advanced Technologies for Producing Solar Cells –

Authors: *Takashi Ishihara\** and *Hiroaki Morikawa\**

## 1. Introduction

Of the total production volume of solar cells categorized by type of raw material, single- and multicrystalline silicon solar cells account for about 90%, with the latter accounting for 60%.

Multicrystalline silicon is the most frequently used material for solar cells because it enables high efficiency and low-cost production using a simple manufacturing process. Various techniques to raise the efficiency of multicrystalline silicon solar cells have been studied for more than 20 years, such as gettering, dry texturing, selective emitters, and hydrogen passivation. However, not all of the techniques are applicable to mass production; only those that are optimized for productivity and equipment cost have been used.

As shown in Fig. 1, the manufacturing process currently used in mass production consists of six subprocesses<sup>(1)</sup>, all of which are essential for manufacturing silicon crystalline solar cells. Among others, hydrogen passivation is indispensable for improving the efficiency of multicrystalline silicon cells. Focusing on hydrogen passivation, this paper reports on technologies and subprocesses such as anti-reflection coating and electrode firing that influence the effects of hydrogen passivation.

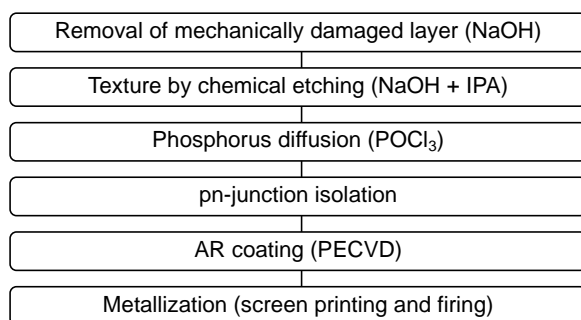


Fig. 1 Fundamental process sequence for the cells

## 2. Technologies for Improving the Efficiency of Solar Cells

### 2.1 Anti-reflection coating and passivation effect

Any thermal process influences the minority-carrier diffusion length (Ld), which is an index for evaluating the quality of multicrystalline silicon wafers. Therefore, it

is important for improving the efficiency to understand the dependency of Ld on the thermal processes. In the process sequence shown in Fig. 1, Ld is influenced by three thermal processes: phosphorus diffusion, plasma-enhanced chemical vapor deposition (PECVD), and electrode firing. Therefore, we assessed the Ld values after each thermal process on three types of wafers made by different manufacturers. The Ld values were assessed using the surface photovoltage (SPV) method after the surface of each wafer was etched at the following four states: 1) initial state (prior to its input in the process); 2) after phosphorus diffusion; 3) after formation of anti-reflection coating; and 4) after electrode firing. Figure 2 shows the relationship between the Ld values and each process. The Ld value decreases after the first thermal process, phosphorus diffusion, for all wafers of all manufacturers. The value recovers slightly after the anti-reflection coating is formed, and then improves significantly after the electrode firing process. The anti-reflection coating is a silicon nitride (SiN) film, which is formed by decomposing silane (SiH<sub>4</sub>) and ammonia (NH<sub>3</sub>) gases using the PECVD method. It is known that the hydrogen atoms contained in the SiN film have a significant effect on the passivation behavior.

With regard to the SiN film which is essential for hydrogen passivation, to determine the required film

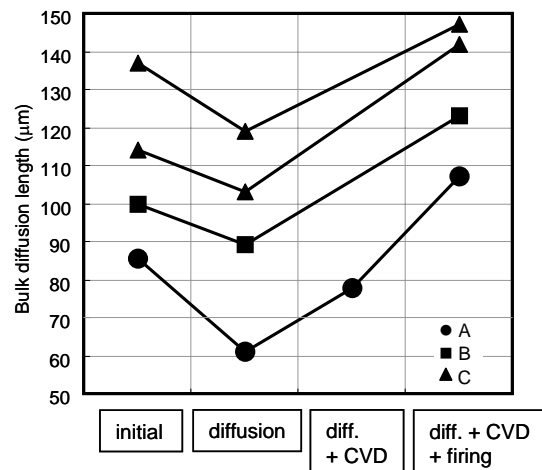


Fig. 2 Change in diffusion length with process steps (A, B, C: suppliers)

thickness to maximize conversion efficiency, we examined the dependence of the internal quantum efficiency (IQE) on the SiN film thickness. Figure 3 shows the relationship between the SiN film thickness and IQE.

In the short wavelength range below 400 nm, an SiN film 35 nm thick gives the maximum IQE value. Previous studies have shown that if an SiN film having a refractive index of 2.2 is 35 nm or thicker, the IQE decreases due to absorption by the SiN film. Meanwhile, in the long wavelength range above 800 nm, the IQE almost reaches its peak at the thickness of 55 nm. These results clearly indicate that 55 nm is a sufficient thickness to maximize the effect of hydrogen passivation. In contrast, the optimum SiN film thickness for a solar cell to prevent light reflection on the surface and maximize the light intensity into the cell, is about 75 nm. According to these results, the optically optimum film thickness (75 nm) differs from the film thickness that maximizes the effect of hydrogen passivation (55 nm). However, if the module structure is also taken into consideration, light below 400 nm barely enters the cell due to absorption by the module's sealing materials, ethylene vinyl acetate (EVA) and strengthened glass, and thus has little influence on the module output. As a result, it was experimentally clarified that the optimum thickness of SiN film is around 75 nm, where the effect of hydrogen passivation is maximized and the reflection is minimized, giving high optical efficiency.

### 2.2 Electrode firing conditions and cell properties

As shown in Fig. 2, the  $L_d$  value is significantly improved after the electrode firing process. To understand

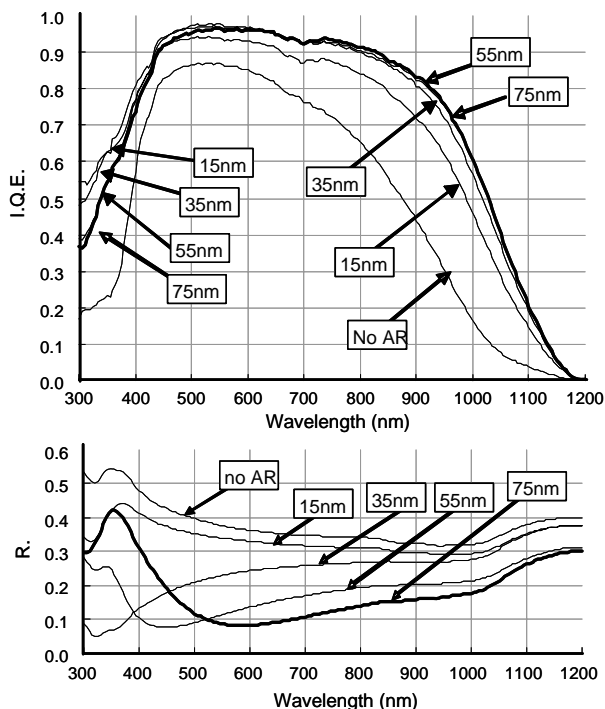


Fig. 3 Dependence of IQE and reflectivity on AR coating thickness

the electrode firing process, we evaluated the change in  $L_d$  resulting from the PECVD and electrode firing processes, both of which improved the value of  $L_d$ . The evaluation was performed by examining IQE values for the following four types of solar cells, and Fig. 4 shows the change in IQE for each type: 1) Anti-reflection coating is not formed, and electrodes are formed using print paste and fired at 800°C or higher ("A" on the chart); 2) Anti-reflection coating is not formed, and electrodes are formed by sputtering and sintered at 300°C ("B" on the chart); 3) Anti-reflection coating is formed, and electrodes are formed by sputtering and sintered at 300°C ("C" on the chart); and 4) Anti-reflection coating is formed, and electrodes are formed using print paste and fired at 800°C or higher ("D" on the chart). In the cases without anti-reflection coating, the IQE for Type B was greater than that for Type A. That is, under the conditions without anti-reflection coating, temperature exceeding 800°C for printed electrodes caused a significant decrease in IQE (gap x).

Meanwhile, after the SiN film was formed, the IQE for Type D where the firing temperature exceeded 800°C was greater than that for Type C that was treated at 300°C. Considering the results for the cases without anti-reflection coating, it is considered that if an anti-reflection coating is not present, the state of Type A results from the influence of temperature, whereas the presence of anti-reflection coating, i.e., the effect of hydrogen passivation, improves the state of A to D (gap y). One explanation for these relationships is that a hydrogen passivation effect is induced by the hydrogen being contained in the anti-reflection coating, and dur-

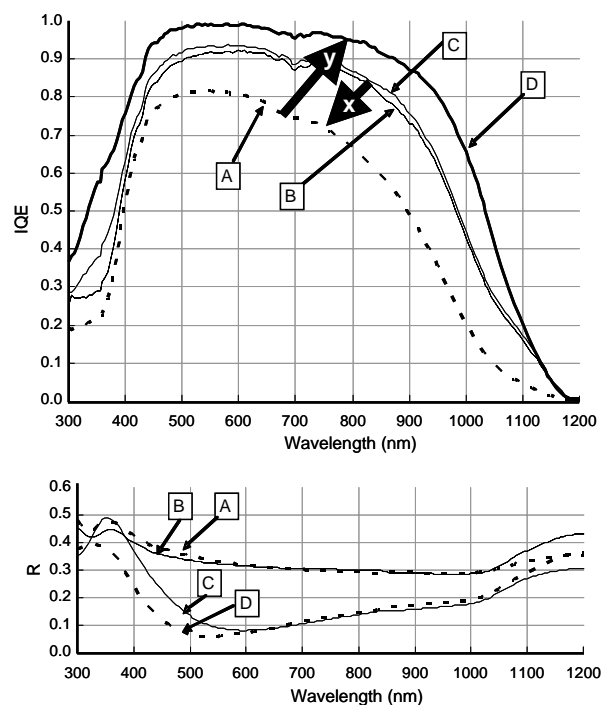


Fig. 4 Effect of metallization process on diffusion length

ing the electrode firing process both deterioration from the heat (gap x) and improvement from the hydrogen passivation (gap y) occur at the same time. It is conjectured that it may be possible to improve  $L_d$  if the cause of gap x (deterioration) differs from the cause of gap y, for example, if at the electrode firing temperature, gap x is caused by the rediffusion of heavy metals segregated along grain boundaries, thus preventing temperature-induced deterioration. Consequently, we worked on a rapid firing process that could maximize the effect of hydrogen passivation.

Figure 5 compares the profiles for the rapid firing and conventional processes. In the experimental rapid firing process, the duration of peak firing temperature was set to a short period of less than several seconds, and the rate of temperature rise/fall was set to  $30^\circ\text{C/s}$  or faster.

Figure 6 shows the relationship between the short circuit current density ( $J_{sc}$ ) and the open circuit voltage ( $V_{oc}$ ) for both the rapid firing and conventional firing processes. For this comparison, we used sister wafers supplied from three different manufacturers (sister wafers: multicrystalline wafers taken from as close positions of an ingot as possible to obtain nearly the same  $L_d$  and other electrical properties). Dotted lines in the chart represent the simulation results of PC-1D

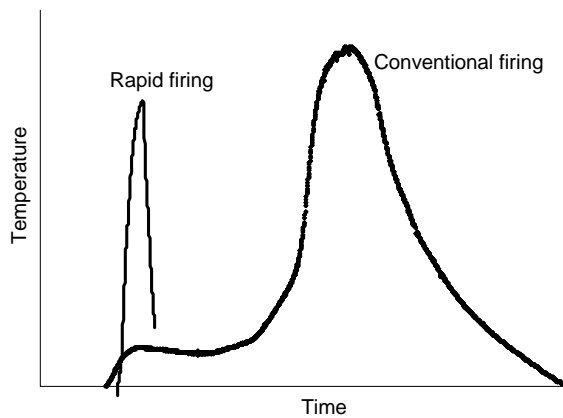


Fig. 5 Comparison of firing profiles

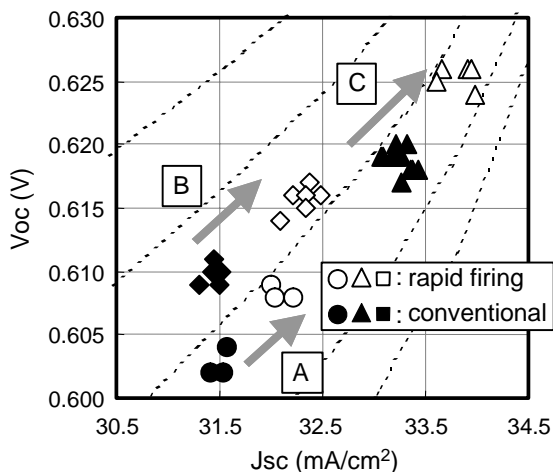


Fig. 6 Enhancement of  $V_{oc}$  and  $J_{sc}$  by rapid firing

(one-dimensional device simulator for solar cells) for the relationship between  $J_{sc}$  and  $V_{oc}$  at various values of resistivity in the case where  $L_d$  is the only single variable parameter. As the  $L_d$  improves,  $J_{sc}$  and  $V_{oc}$  also simultaneously improve. With any set of sister wafers (A, B or C) from different manufacturers, both  $J_{sc}$  and  $V_{oc}$  were improved by changing from the conventional to rapid firing process, and the pattern of improvement was the same as that for the PC-1D simulation results. These results confirmed that rapid firing improves the diffusion length,  $L_d$ .

Meanwhile, Fig. 7 shows the relationship between the product of  $J_{sc}$  and  $V_{oc}$  and the distance from the top side of each ingot toward the bottom side. This chart also compares the rapid firing and conventional processes from the results obtained using the sister wafers. Since the wafers close to the top side of the ingot showed a significant improvement, it is inferred that rapid firing effectively inhibits the rediffusion of heavy metals segregated at the top side of each ingot.

In order to ensure high efficiency and reliability under these new rapid firing conditions, we simultaneously worked on optimizing the front-surface electrode (Ag paste). To improve the efficiency, a finer line width of the grid electrode has a direct advantage for increasing the input light intensity. We achieved a grid line width of  $60\ \mu\text{m}$  by applying the multiple printing technique, optimizing the viscosity and other rheological parameters of metal paste, and optimizing the screen printing parameters including mesh size and mesh count, and screen mask conditions such as emulsion thickness, printing pressure, and mask-wafer gap.

For improved reliability using this process sequence, it is essential to optimize the Ag paste for the front-surface electrode and the firing conditions. For reliability, we worked on optimizing the process conditions for rapid firing, and successfully achieved better reliability than the previous process.

In addition to the described technologies for improving solar cells: hydrogen passivation, rapid firing,

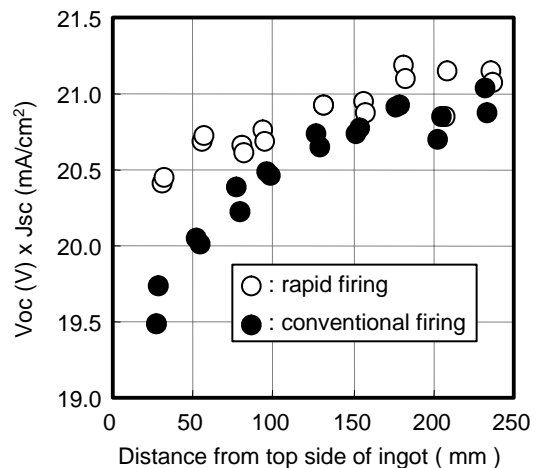
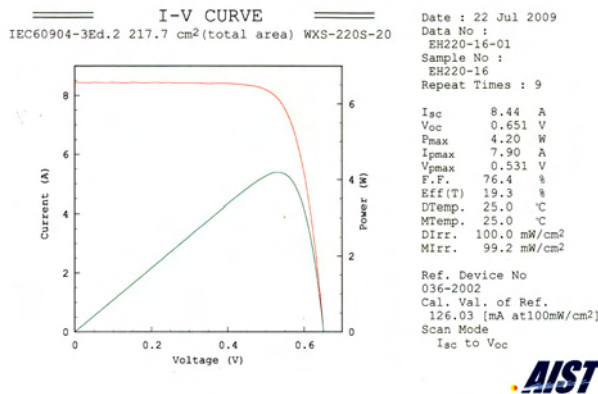


Fig. 7 Enhancement  $V_{oc} \times J_{sc}$  (life time) by rapid firing

and finer line width for the front-surface electrode, we made additional improvements (to be reported elsewhere) for the multicrystalline silicon solar cells including honeycomb texture, high sheet-resistance ratio for emitter layer, rear surface point contact, and rear surface reflection structure. Furthermore, as shown in Fig. 8, we successfully achieved a conversion efficiency of 19.3% with a practical 150 mm square multicrystalline silicon solar cell.

### 3. Conclusion

This paper described the technologies for improving the efficiency of crystalline solar cells. We are confident that by applying new efficiency-improvement technologies already proven at the research level and optimizing the resistivity of wafers, we can also further improve the efficiency of crystalline silicon solar cells suitably configured for mass production with the bus and grid lines formed on the front surface.



### References

- (1) S. Arimoto et al: Simplified mass-production process for 16% efficiency multi-crystalline Si solar cells, Proceedings of the 28th IEEE Photovoltaic Specialists Conference, Anchorage, 2000, p. 188-193.

| Jsc (mA/cm <sup>2</sup> ) | Voc (V) | F.F.  | Eff (%) |
|---------------------------|---------|-------|---------|
| 38.80                     | 0.651   | 0.764 | 19.3    |

Fig. 8 I-V characteristics independently measured at AIST

# Energy Conservation and Resource Saving via SiC Inverters

Authors: *Shin-ichi Kinouchi\** and *Shuhei Nakata\**

## 1. Introduction

It is estimated that widespread use of silicon carbide (SiC) devices could yield energy savings equivalent to 83 million tons of CO<sub>2</sub> reduction by 2030<sup>(1)</sup>. Mitsubishi Electric Corporation is working to develop SiC devices and their application technologies, and to introduce them quickly to help conserve energy and material resources.

## 2. Fabrication of Prototype 3.7-kW Class SiC Inverter

The use of SiC realizes unipolar devices with high voltage blocking capability, which can significantly reduce switching loss during on/off switching of the device. It is difficult to create such devices for practical applications by using Si.

Mitsubishi Electric Corporation is working to develop unipolar devices, SiC metal oxide semiconductor field effect transistors (MOSFETs) and SiC Schottky barrier diodes (SBDs), and to put these SiC devices into practical use by improving their fundamental characteristics and developing the application technologies for module fabrication and converter control.

In FY2007, we fabricated a prototype 400-V/3.7-kW SiC inverter to confirm the low loss performance of the SiC device for converter applications.

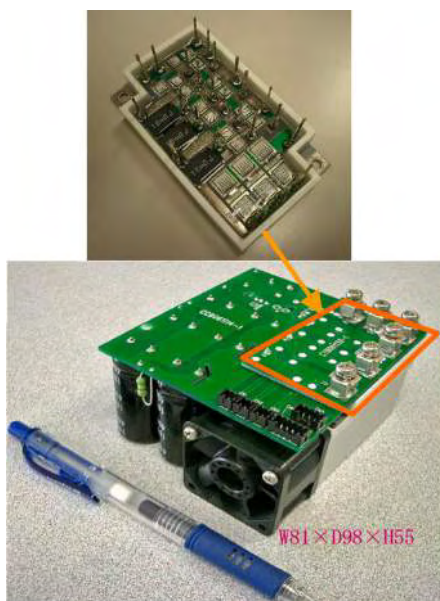


Fig. 1 400-V/3.7-kW class SiC inverter (lower) and SiC module (upper)

Since a switching test conducted in advance predicted an operating power loss of 50% or lower than that of a conventional Si inverter, we designed the SiC inverter with a target power density of about four times greater than that of a similarly rated Si inverter. If both Si and SiC inverters have the same basic fin structure made of the same pure aluminum material, the low loss advantage of the SiC device could reduce the volume of forced air cooling systems by 65% (the total volume of the air cooling fan and fins).

Figure 1 shows the prototype 400-V/3.7-kW class SiC inverter and SiC module. Overall dimensions of the SiC inverter are 81×98×55 mm and the power density is about 9 W/cm<sup>3</sup>.

To evaluate the performance, a 400-V/3.7-kW motor was driven by the experimentally assembled 3.7-kW class SiC inverter. Using a carrier frequency of 10 kHz and output of 3.7 kW, the power loss of the SiC inverter was less than 50% of that of the Si inverter. Note that the power loss values of the Si inverter used for the comparison were calculated by evaluating its forward I-V characteristics and transient characteristics.

Figure 2 shows the dependency of inverter power loss on the carrier frequency of pulse width modulation (PWM) at an output level of 3.7 kW. The power loss of SiC at the carrier frequency of 15 kHz is nearly the same as that of Si at 5 kHz, and the advantageous effect of reduced switching loss is obvious.

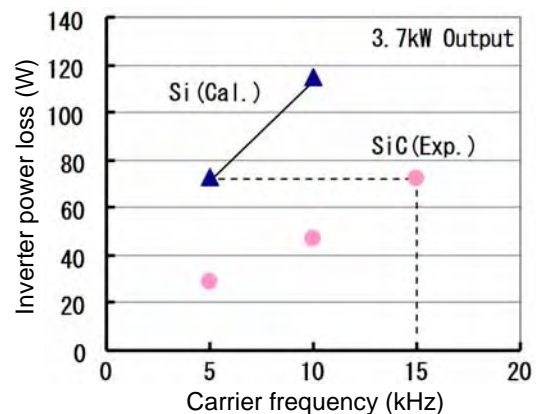


Fig. 2 Dependency of inverter power loss on PWM carrier frequency at 3.7 kW output

### 3. Fabrication of Prototype 11-kW SiC Inverter

In FY2008, we fabricated a prototype 400-V/11-kW class SiC inverter as shown in Fig. 3. This SiC inverter has a volume of 1.1 L and thus a power density of about 10 W/cm<sup>3</sup>, which is about four times greater than that of a similarly rated Si inverter.

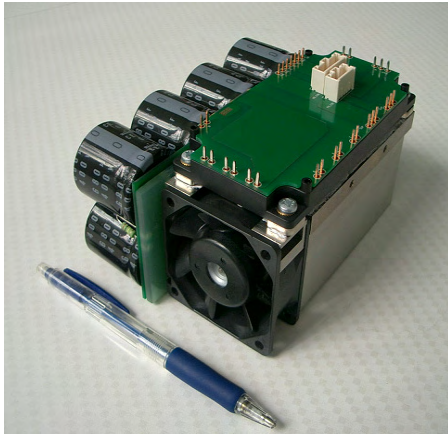


Fig. 3 400-V/11-kW class SiC inverter

The operating power loss of the SiC inverter calculated by evaluating its forward I-V characteristics and transient characteristics was 70% less than that of the conventional Si inverter. The calculation conditions were as follows: carrier frequency 15 kHz; power factor 0.8; effective current 23 A; and junction temperature 125°C. The reduction in switching loss is significant: the switching loss itself is reduced by 83%.

The potentially significant reduction in switching loss suggests that the SiC inverter would be advantageous for high-frequency applications. Figure 4 shows the dependency of inverter power loss on the PWM carrier frequency at an output level of 11 kW. The power loss of SiC at a carrier frequency of 30 kHz is lower than that of Si at 5 kHz. If the carrier frequency could be increased by six fold using a high power factor

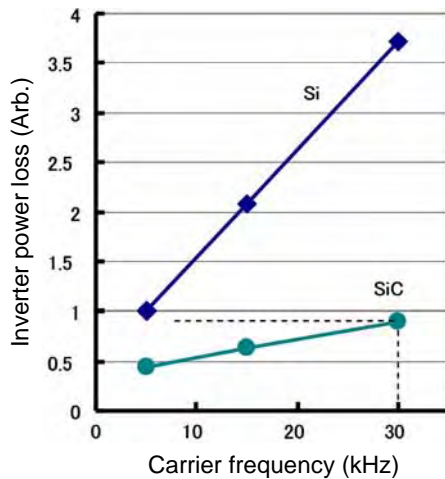


Fig. 4 Dependency of inverter power loss on PWM carrier frequency at 11 kW output

converter, distributed generation converter, etc., the filter reactor could be drastically reduced.

A 400-V/11-kW motor was driven by the experimentally assembled 11-kW class SiC inverter. Using a carrier frequency of 15 kHz and output of 11 kW, stable inverter operation was confirmed.

### 4. Ultra-low Loss 400-V/22-kW Class SiC Inverter

In 2010, we fabricated a prototype ultra-low loss 400-V/22-kW class SiC inverter to check the limit for reducing power loss with the SiC inverter. Figure 5 shows an external view of the prototype inverter and the inside of the SiC module.

An effective way of reducing the SiC inverter loss is by using a high-speed drive for the SiC device, which reduces the switching loss by shortening the switching time. However, due to the parasitic inductance within the inverter circuit, a surge voltage is generated and the high-speed drive has a certain upper limit. For the ultra-low loss 22-kW class SiC inverter, we reduced the parasitic inductance of the inverter circuit to 6 nH by optimizing the device configuration and wiring pattern.

We evaluated the transient characteristics of the 22-kW class SiC inverter by using a newly developed high-speed drive technology, and then calculated the operating power loss of the inverter from those evaluation results. The calculation conditions were as follows: carrier frequency 20 kHz; effective current 43 A; and junction temperature 125°C. Compared to the conventional Si converter, power loss was reduced by 90%.

An operational test was performed on the experimentally assembled 22-kW class SiC inverter by driving a 400-V/22-kW motor, and stable rated operation was confirmed.

### 5. Conservation of Energy and Material Resources by Using SiC Inverters

Power devices are used in a wide range of applications, and SiC devices are also expected to be used in a variety of appliances. If all inverters for air conditioners and refrigerators currently used in Japan are replaced with SiC inverters, the resulting energy saving

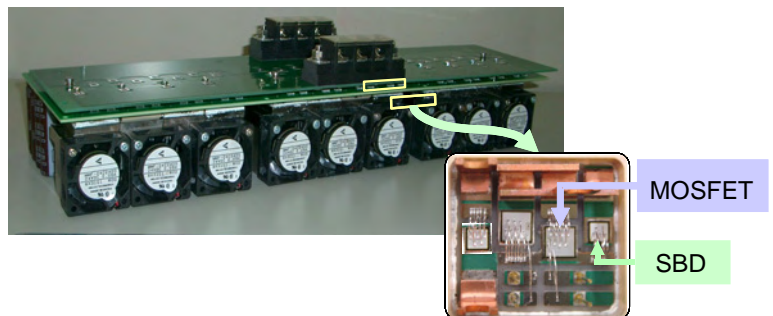


Fig. 5 Ultra-low loss 400-V/22-kW class SiC inverter and SiC module

effect would be equivalent to one million tons of CO<sub>2</sub> reduction. While the power converters used in photovoltaic power generation systems have reached an efficiency of about 97.5%, the efficiency could be raised almost to 99% by using SiC devices. It is also estimated that SiC inverters could improve the fuel mileage of rapidly spreading hybrid cars by about 10%<sup>(1)</sup>.

Mitsubishi Electric Corporation has been working to develop SiC devices as well as their application technologies, and as shown in Fig. 6, successfully demonstrated their reduced power loss when applied to

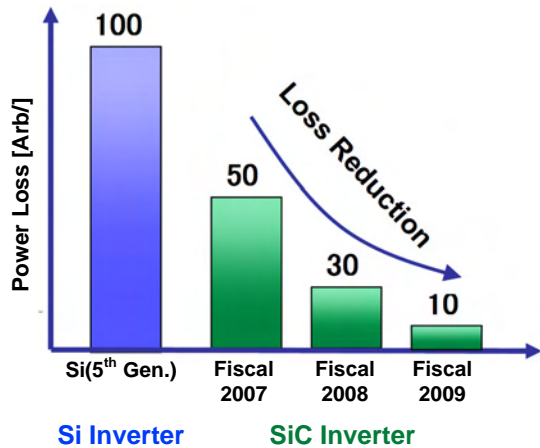


Fig. 6 Progress in power loss reduction of SiC inverter by MELCO

inverters<sup>(2), (3)</sup>. The widespread use of SiC devices is expected to dramatically contribute to conserving energy and material resources, and efforts are being made to introduce these devices at an early date. For practical and widespread use of SiC inverters, while it is important to enhance their performance and reduce the cost, it is also important to establish reliability technologies and investigate how to optimize the advantages of SiC devices depending on the characteristics of the equipment in which the SiC inverters are to be installed.

Part of this research study is the outcome of the project "Development of Inverter Systems for Power Electronics" commissioned by the Ministry of Economy, Trade and Industry and the New Energy and Industrial Technology Development Organization (NEDO).

### References

- (1) Report for the Council on Competitiveness – Nippon (COCN): Green Power Electric Technologies (2009) (in Japanese)
- (2) Kinouchi, S., et al.: High Power Density SiC Converter, Material Science Forum Vols. 600–603, 1223–1226 (2009)
- (3) Nakata, S., et al: Substantial Reduction of Power Loss in a 14 kVA Inverter Using Paralleled SiC – MOSFETs and SiC-SBDs, Silicon Carbide and Related Materials 2008, 903–906 (2009)

# Lineup and Features of Air-to-Water Products for Europe

Author: Yoshihiro Takahashi\*

## 1. Introduction

The demand for energy-saving heating systems has increased in Europe much faster than expected. This is due to the need for CO<sub>2</sub> emissions reduction, environmental preservation and energy compensation, the trend toward cutting energy costs (saving energy), stricter regulations on energy saving, and various incentives for purchasing energy-saving equipment in each country. Mitsubishi Electric Corporation has, using its heat pump technologies developed for air conditioners, created air-to-water (ATW) heat pump heat source units and interface units. The ATW unit utilizes the heat of air instead of conventional combustion boilers (gas, oil, etc.) and serves as a heat source for radiator heating, floor heating and hot water supply systems, which are commonly used in Europe, while the interface unit enables the construction of a total heating system that works together with the customer's other local units. This article describes these products.

## 2. ATW System in Europe

In Europe, the most commonly used heating system is a radiant heating type: hot water is heated by a boiler or heat pump and supplied to radiators and the floor heating system. Figure 1 shows a typical ATW system configuration in Europe.

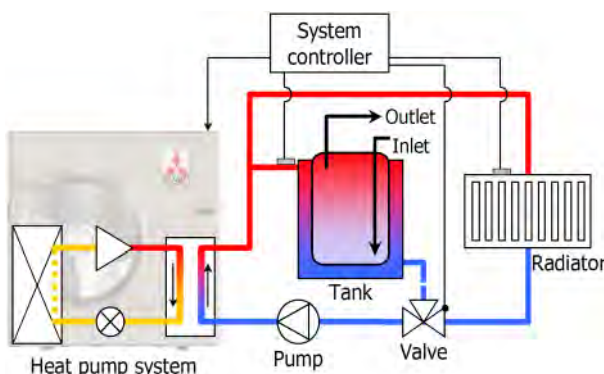


Fig. 1 Typical ATW system in Europe

### (1) Configuration of heating system circuits

The hot water supply tank is either a dual type or with a built-in heater coil, and the domestic water and heating water circulating through the heat pump are separated. The domestic water circuits and heating circuits are connected in parallel. The water is heated by the heat pump (or boiler) and switched by a valve to

be supplied into either of the two circuits. During typical operation in the morning, the water supply tank is heated to keep domestic hot water, then during the daytime the hot water is supplied to the heating system. A system controller controls the whole system monitoring the water and room temperatures and controlling the heat pump as a heat source, and the pumps and valves in the water circuits.

### (2) Types of outdoor units of heat pumps

The ATW heat pump systems used in Europe can be divided into two main groups depending on the type of outdoor unit: the all-in-one type and the split type, as shown in Fig. 2. The all-in-one type outdoor unit has a built-in water heat exchanger, and most European manufacturers have adopted this type. One advantage of this type is that no refrigerant piping is required and the system can be installed using only the city water plumbing. On the other hand, the split type has no water heat exchanger inside the outdoor unit, and instead requires a unit called a hydrobox that has a built-in water heat exchanger. Most Japanese manufacturers have adopted this type, because a standard outdoor air conditioner unit can be diverted for use in this system. This system requires, in addition to city water plumbing, refrigerant piping work the same as for a normal air conditioner.

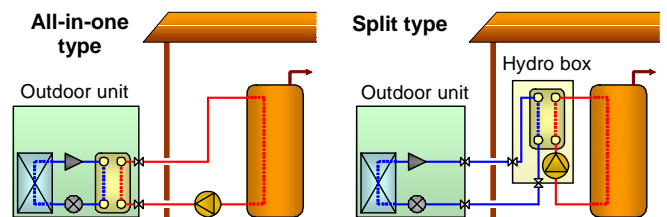


Fig. 2 Types of ATW outdoor unit

## 3. Effectiveness of ATW Heat Pump

We installed a Mitsubishi Electric ATW heat pump system (heating capacity of 8.5 kW) in a detached house in the U.K., and carried out a demonstration test from October to November 2007 to verify the energy-saving effect. Figure 3 shows the layout of the radiators and floor heating of the house where the test was performed, and Table 1 shows the measurement results. As shown in the table, the heat pump system effectively saved energy: CO<sub>2</sub> emissions were reduced by 49% and running cost by 39% compared with the previously used gas boiler system.

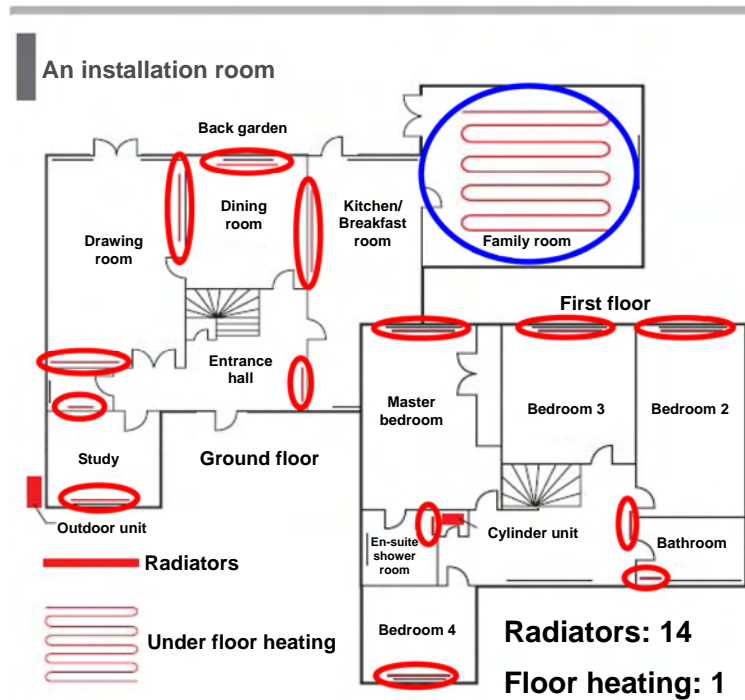


Fig. 3 House layout for demonstration test

Table 1 Demonstration test results

Actual operation data measured from October to November 2007  
Actual measurement of specifications

|                                |                       |            |
|--------------------------------|-----------------------|------------|
| Total                          | Heating power         | 2,216      |
|                                | Elec power (kWh)      | 630        |
|                                | COP                   | 3.52       |
|                                | Cost (£)              | 53.55      |
| Ambient temperature (°C)       | min                   | 3.4        |
|                                | avg                   | 7.2        |
|                                | max                   | 11.4       |
| Room temperature               | min                   | 19.7       |
|                                | avg                   | 21.1       |
|                                | max                   | 22.5       |
| CO <sub>2</sub> emissions (kg) | Heating power         |            |
| Heat pump                      | @0.43 kg per kWh      | 270.9      |
| Old gas boiler                 | 80%, @0.19 kg per kWh | 526.3      |
| Saving                         |                       | <b>49%</b> |
| Run cost savings               |                       |            |
| Heat pump                      | (8.50 p/kWh)          | 53.55      |
| Old gas boiler                 | Eff 80% (3.18 p/kWh)  | 88.1       |
| Saving                         |                       | <b>39%</b> |

\* Electric fee and gas fee as of December 2007

## 4. Product Features

### 4.1 Product line-up

In 2007, Mitsubishi Electric Corporation developed an all-in-one type ATW unit with a heating capacity of 8.5 kW and entered the ATW business. Since then, the company has extended its range of outdoor units by adding new 5.0 kW, 11.2 kW and 14.0 kW all-in-one models, as well as split-type models: the Power Inverter Series with a high coefficient of operation (COP) and high heating capacity, and the "Zubadan" Series with even better heating capacity especially at low outdoor temperatures for use in northern countries. (Features of the Zubadan technologies are described in section 4.2.)

Table 2 shows the 2009 product range of ATW heat pump outdoor units.

### 4.2 High heating capacity

Figure 4 shows the refrigerant circuit of a typical model in the Zubadan Series, the all-in-one 14.0 kW model. As described above, the Zubadan series offers improved heating capacity at low outdoor temperatures. In this series, a weakness of the heat pump, i.e. the decrease in heating capacity at low outdoor temperatures, was overcome by using the technologies described below.

This unit has various technical features including a flash injection circuit, injection compressor using a

high-efficiency DC motor, and power receiver + twin LEVs (electric expansion valve). In the flash injection circuit, heat exchange of the refrigerant is performed in the Heat Inter Changer (HIC) circuit; as a result, the refrigerant is converted from the liquid phase to the vapor/liquid two-phase state before being returned to the injection port of the compressor. This achieves a high heating capacity and superior energy-saving effect even at low outdoor temperatures by keeping a sufficient amount of refrigerant in circulation. In addition to the LEVs located before and after the power receiver, the LEV-C is installed in the injection line, and these LEVs control the operation to optimize the condition of the refrigerant according to the load condition and operation mode. The subject and method of LEV control during this injection heating operation are shown in Fig. 5.

Figure 6 shows how the heating capacity characteristics vary with outdoor temperature (when the hot water outlet temperature is 35°C). While the heating capacity of the heat pump system normally decreases as the outdoor temperature lowers, the Zubadan avoids this decrease by means of injection, and thus successfully overcomes its disadvantage compared with a boiler system, which maintains a constant capacity regardless of outdoor temperature.

### 4.3 Improvement of heating efficiency at low temperatures

Generally, when the heat pump is running for heating operation, as the outdoor temperature falls the heat exchanger becomes frosted and the COP is significantly lower than that at high outdoor temperature where frost does not form. Since the ATW unit is mainly used for heating, it is designed to be more suitable for heating than regular air conditioners which serve for

both cooling and heating. The key technologies implemented in this custom designed ATW unit are:

- (1) Dual stage heat exchanger: In the upstream side of the multi-row heat exchanger where more frost forms, the fin pitch is increased to equalize the amount of frost on each row and hence slow down the decrease in efficiency due to clogging of the heat exchanger with frost.
- (2) Heat exchanger design focusing on heating function: The heat exchanger, which works as an evaporator, is designed so that the number of passes and pass pattern are optimized for heating. As a result, the heat exchange property is improved and the pressure loss is reduced.
- (3) While the compressor is in defrosting mode, the operation frequency is reduced to an optimum level, resulting in a lower input power to the compressor and thus a higher COP during defrosting.
- (4) The resistance of refrigerant circuits is reduced by enlarging the LEV diameter. As a result, the amount of refrigerant in circulation is increased during defrosting, thus improving defrosting performance, shortening the defrosting time, and achieving a higher COP during defrosting operation.

### 4.4 Development of interface

As previously described, the whole ATW system is controlled by the system controller, and the heat pump outdoor unit operates in response to commands from the controller. An actual setup, however, requires an interface for communications between the customer's

Table 2 Lineup of ATW outdoor units

|                 |                | 2HP | 3HP | 4HP | 5HP | 6HP | 8HP | 10HP |
|-----------------|----------------|-----|-----|-----|-----|-----|-----|------|
| All-in-one type | Power inverter | ○   | ○   |     |     |     |     |      |
|                 | Zubadan        |     |     | ○   | ○   |     |     |      |
| Split type      | Power Inverter | ○   | ○   | ○   | ○   | ○   | ○   | ○    |
|                 | Zubadan        |     | ○   | ○   | ○   |     | ○   |      |

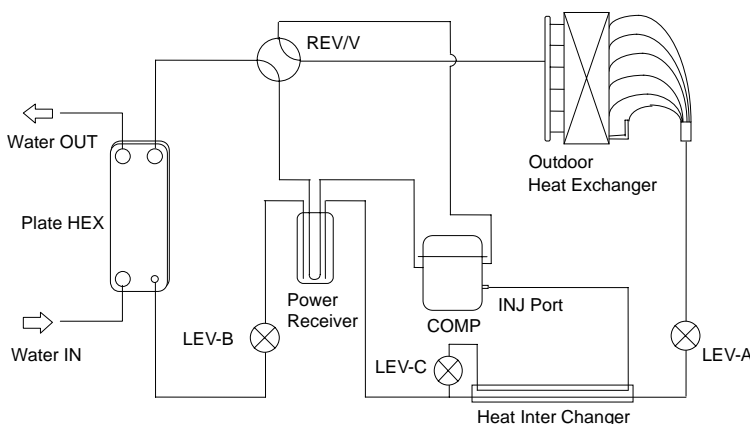


Fig. 4 Refrigerant circuit

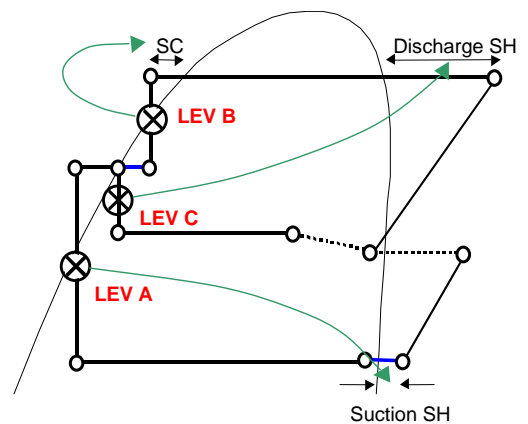


Fig. 5 LEV control during injection operation

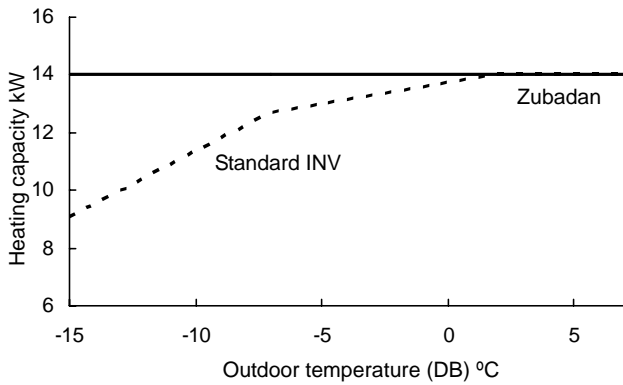


Fig. 6 Heating capacity characteristics of Zubadan

local system controller and our heat pump outdoor unit. Mitsubishi Electric therefore developed such an interface unit in parallel with the outdoor unit, and built various types of interface units depending on the customers and applications, thus boosting sales channels for the outdoor units.

(1) I/F (Type name: PAC-IF011B-E)

The I/F receives operation mode and performance step (0–7) signals from the system controller, and then transmits the request mode and performance data to the outdoor unit after converting them to Mitsubishi Electric’s own A control signals (Fig. 7). Note that when building a system using the I/F, vendors must have relatively advanced technologies to build a system for controlling the performance of the heat source.

(2) FTC (Type name: PAC-IF021B-E)

The FTC receives only operation mode signals from the system controller. It acquires the hot water outlet temperature and controls the frequency of the

outdoor unit so that its outlet temperature reaches the target temperature set by remote control (Fig. 8). Even if the system controller is unable to control the heat pump performance, the inverter outdoor unit can be controlled, and so even a technologically unskilled vendor can build a system.

(3) FTC2 (Type name: PAC-IF031B-E)

The FTC2 acquires temperature data from the tank and the hot water outlet in the water circuits, and controls each component in the water circuits (Fig. 9). Since the FTC2 makes it possible to control the outdoor unit as well as each component in the water circuits without a system controller, an ATW system can be built merely using the FTC2 and remote controller.

5. Conclusion

In 2007, we started by successfully developing the ATW-dedicated outdoor unit and entered the ATW business. We have since developed additional outdoor units and interface models, and our product lineup now covers most market needs. Looking ahead, in order to survive the severe competition with other manufacturers, we need to improve the fundamental performance including energy-saving properties, which is the highest priority for the ATW unit, and reduce the noise level of the outdoor unit to expand home use applications. We also need to consider differentiation such as strengthening our advantages. We will continue to develop products that contribute to business expansion by working closely with other divisions including: developing new technologies with research laboratories, gathering and examining local information, and product planning with marketing and sales divisions.

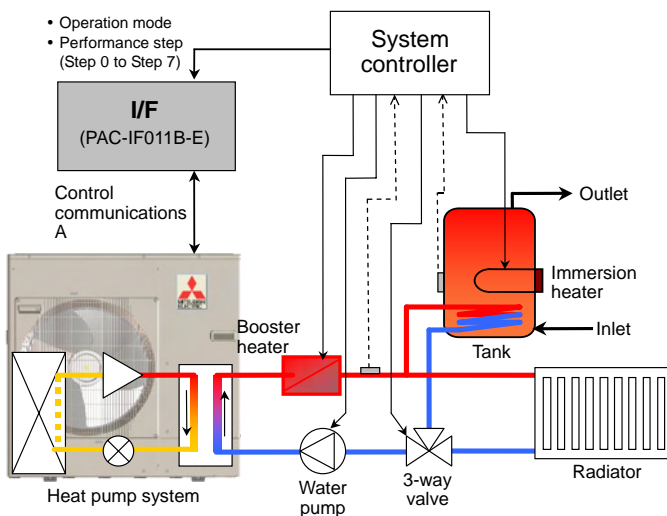


Fig. 7 ATW system with I/F

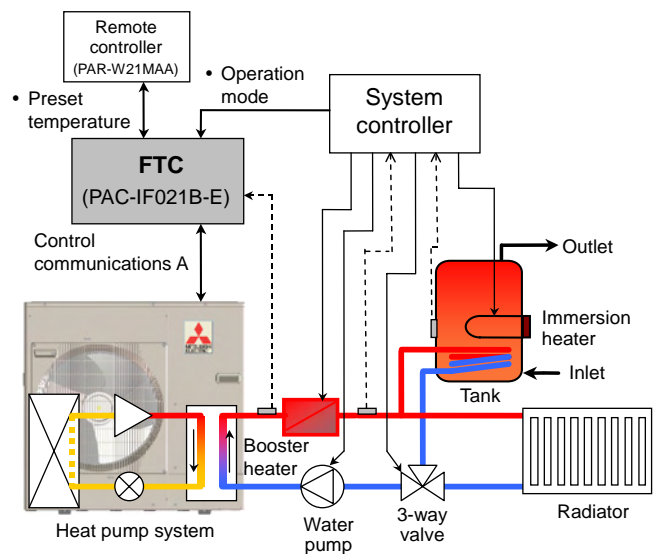


Fig. 8 ATW system with FTC

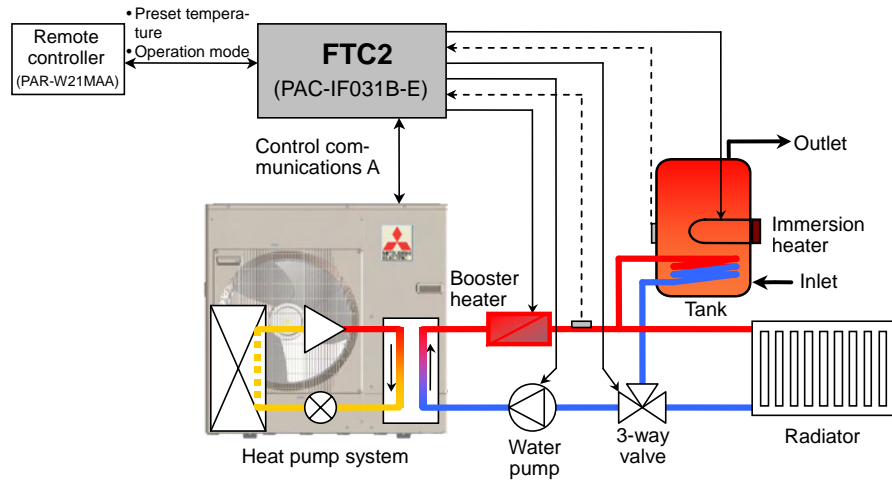


Fig. 9 ATW system with FTC2

